10,11

Investigation of structural features of natural disordered carbon by texture analysis of electron microscopy images

© I.V. Antonets[1], V.A. Ustyugov[1], E.A. Golubev[2]

[1] Pitirim Sorokin Syktyvkar State University,
Syktyvkar, Russia
[2] Institute of Geology of the Komi Scientific Research Center of the Ural Branch of the Russian Academy of Sciences,
Syktyvkar, Russia

E-mail: ustyugovva@gmail.com

Received April 30, 2025
Revised September 8, 2025
Accepted November 11, 2025

A methodology for automated analysis of shungite transmission electron microscopy images is described. The method is based on the use of information-theoretic entropy as a metric for distinguishing textures in image fragments. Using the developed algorithm, a qualitative and statistical analysis of the structural composition of shungite samples was carried out.

Keywords: natural disordered carbon, electron microscopy, structural entropy, image segmentation.

DOI: 10.61011/PSS.2025.12.63116.8048k-25

Natural and synthetic materials, which are forms of disordered carbon, have many attractive properties for industrial and technological applications. These include high electrical conductivity (due to the presence of graphite-like structural elements), chemical stability and catalytic activity, resistance to high temperatures and aggressive environments [1–8]. An example of naturally occurring disordered carbon is the rock shungite, common in Karelia (Russia) and used in metallurgy to improve the quality of cast iron and steel, in the chemical industry as an adsorbent, for soil reclamation. A developing and promising area is the use of fullerene-like structures of shungite in nanoelectronics and medicine. However, its use is often limited by the need for additional processing and insufficient standardization of the quality of raw materials.

Currently, the relationship between the functional properties of shungite and its structure is being actively studied. The carbon component of a shungite rock can be formed as curved graphene layers in various spatial configurations, that is, forming compact bundles, extended ribbons, and globules [9,10]. The most convenient method for studying such a complex structure is high-resolution transmission electron microscopy (HREM) [11,12]. The clearly defined alternating light bands in the HREM images of shungite are interpreted as geometric projections of graphene layers (example in Figure 1, *a*). The high complexity of the resulting image (variations in the size of structural elements, their mutual intersections and overlaps in the projection of elements located at different depths relative to the surface, etc.) necessitates the development of a technique for automated processing of HREM images of shungite.

In our early research, algorithms for recognizing micro- and nanoscale conductive and non-conductive phases and estimating their distribution for naturally occurring disordered carbon using two- and three-level sampling methods were developed [13,14]. However, the structural elements in these studies were determined manually („by eye"), which excludes stable repeatability of the results.

This paper is devoted to the automated analysis of HREM images of naturally occurring disordered carbon using image segmentation technology by analyzing the values of the texture metric of their fragments. The HREM images were obtained near the Gauss focus of an objective lens (Brydson, 2011) in an FEI Titan Themis 200−80 transmission electron microscope operating at 80−200 kV and provided with a spherical aberration corrector (CM) and an FEI Ceta 16M CMOS camera. Thin plates for studies were prepared from crushed shungite particles by mechanical thinning followed by ion beam finishing grinding in Gatan PIPS Model 691.

The method of image preprocessing (filtering, background gradient heterogeneity elimination, etc.) and the algorithm for selecting structural elements based on the template search method are described in Ref. [15]. It also shows that the template search does not give satisfactory results due to the high variability of the shapes of the desired elements.

The general algorithm used in this study consists of the following steps: (i) splitting the image into fragments; (ii) calculating a metric characterizing the texture in each fragment; (iii) segmenting the microscopy image based on a matrix of metric values; (iv) calculating statistical characteristics for a variety of selected structural elements. Let's describe the steps in more detail.

(i) The original HREM images are converted to an 8-bit format (the values of each pixel in the range [0−255]). The size of the original map of the sample area was 40×40 nm (1600×1600 pixels), which, when divided into 40×40 cells, corresponds to the size of one cell $1 \times 1\,\text{nm}^2$. The selected area is consistent with the characteristic width of the carbon layers (~ 0.34 nm for graphite-like structures).

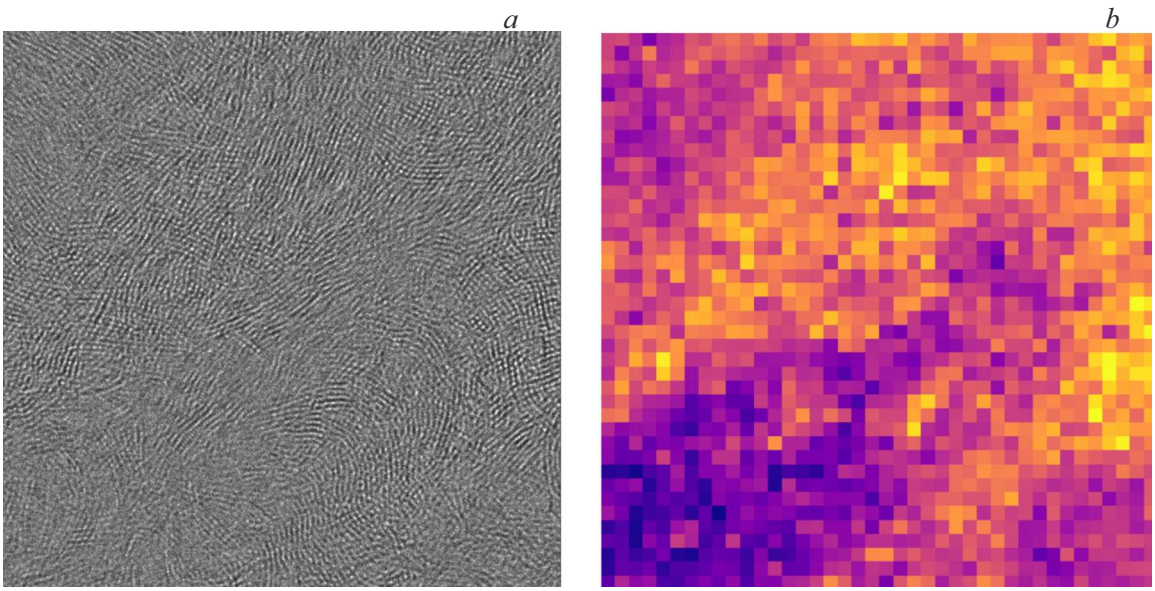

Figure 1. A HREM image of a shungite sample (a) and the entropy matrix of this image (b).

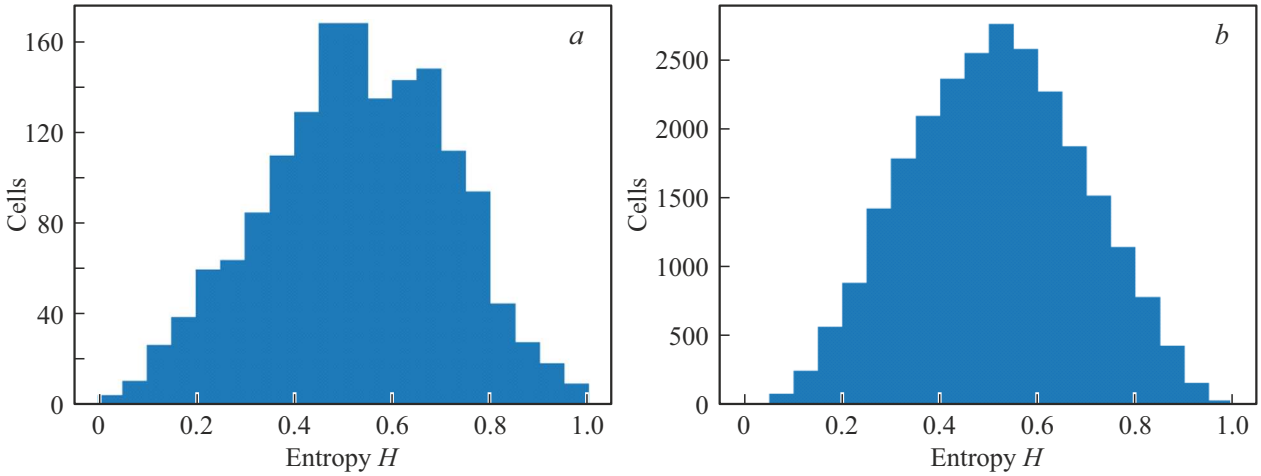

Figure 2. Histogram of the occurrence of entropy values for shungite HREM maps with sizes 40×40 nm (a) and 100×100 nm (b). A small map is a fragment of a large one.

(ii) Information-theoretical entropy (hereinafter referred to as „entropy“) was chosen as the metric characterizing the texture in a cell, which was calculated from the histogram of the pixel intensity distribution in each cell using the formula

$$H = -\sum_{i=0}^{255} p_i \log_2(p_i),$$

where p_i is the occurrence of a pixel with brightness in an image fragment i. Cells corresponding to areas of the sample with an amorphous carbon phase, pores, or defects have a noise content with a small range of values at the pixel level, which corresponds to a low entropy value. On the contrary, if there are contrasting graphene layers in the cell, the entropy value will be high, since the image contains pixels that are close in value to both white and black. It should be noted that from a physical point of view, this fact may seem counterintuitive, but the entropy of an information source that outputs values from a small range, defined in information theory, is lower than in the case of a wider range, provided that in both cases the source messages contain noise.

The entropy values were normalized to 1 to simplify further analysis. An example of the processed image of HREM shungite and the characteristic appearance of the entropy matrix of this sample is shown in Figure 1.

The yellow-tinged cells in Figure 1, b correspond to areas of the HREM image with a high degree of structure (the entropy value is close to 1); the blue and dark purple colors correspond to cells with noise content. Comparing Figure 1, b with the source map, it can be seen that the algorithm determines with high efficiency areas with

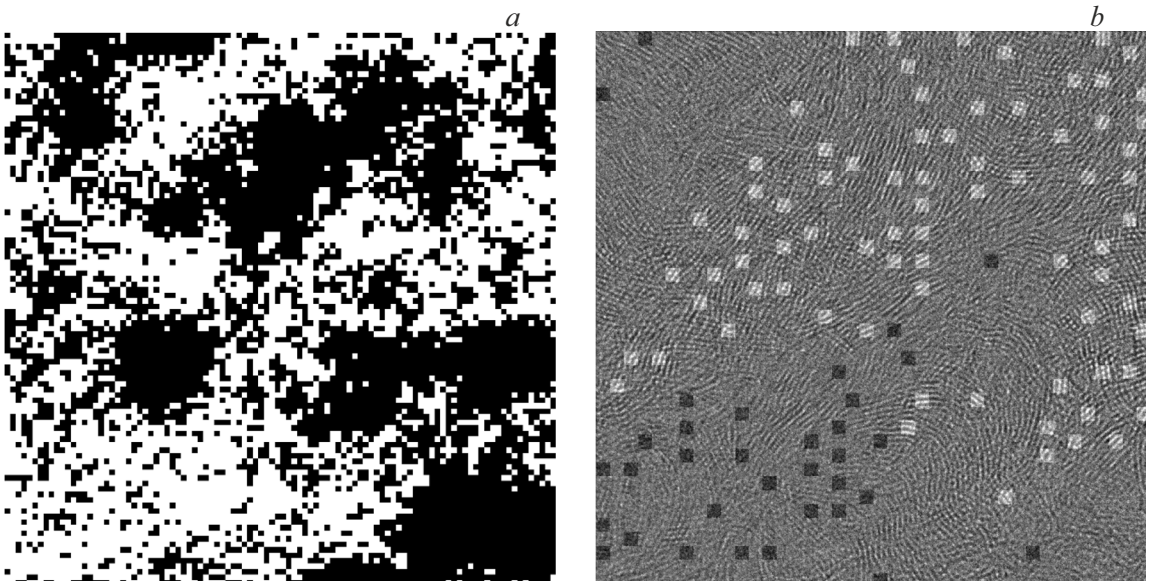

Figure 3. Segmented pores on a map of size 100×100 nm (a); a map of size 40×40 nm with highlighted areas of local maxima and minima of entropy (b).

disordered structure (hereinafter — DOA), for example, in the lower left corner of the image, as well as areas with maximum structure.

The distribution of entropy values by frequency of occurrence can be used as a measure of the structurality and/or uniformity of the sample. Figure 2 shows the corresponding histograms: on the left for a sample map of size 40×40 nm (originally Figure 1, a) and on the right — for a map of size 100×100 nm, with the small map being a fragment of the large one.

Comparing the two histograms, it can be seen that entropy as a metric is local in nature. The distribution in Figure 2, a has an asymmetric character with an additional peak in the region of high entropy values, which indicates its heterogeneity, that is, the presence of both areas with disordered structure and highly structured areas with a predominance of the latter. The histogram obtained from the complete sample map (Figure 2, b) is more symmetrical, which indicates a uniform distribution of areas with disordered structure and structured elements in the natural material of the sample.

(iii) Image segmentation is the division of an image into fragments with qualitatively different contents. In this case, the natural segmentation mechanism consists in allocating cells with an entropy value within a certain range into separate regions. It was stated above that the algorithm effectively defines shungite areas with disordered structure. So, by setting the threshold value of entropy $H = 0.55$ (that is, by redefining the cells in which $H < 0.55$ are black, the rest are white) elongated partially oriented areas with disordered structure of the order of 40 nm in length can be detected in the image of 100×100 nm (Figure 3), the presence and properties of which are probably related to the conditions of formation of shungite.

(iv) Using the method of searching for local maxima by matrix values (and additional filtering by entropy value $H > 0.75$), cells corresponding to the central regions of the structural elements were identified. So, 76 similar cells were found on the fragment of map 40×40 nm (highlighted in Figure 3, b in light color). 455 such cells were found on the complete map 100×100 nm, which is consistent with the histogram data in Figure 2 (an increased percentage of structured cells on a small fragment of the map). Fragments corresponding to local entropy minima are highlighted in a darker color in Figure 3, b. It can be seen that they are located in areas with a lower structure, which positively characterizes the effectiveness of the methodology used. It should be noted, however, that other existing structural metrics can be used to reduce the percentage of false results in determining poorly structured areas.

The issue of complete differentiation on maps and identification of types of structural elements remains open at the moment.

The developed HREM image analysis method and the data obtained in this study can be used to develop models of shungites as continuous media and determine the mechanisms of the relationship between the internal structure of shungites and macroscopic (for example, electrodynamic) properties.

Funding

The study was carried out within the framework of the state assignment of the„Pitirim Sorokin SSU“ No. 075-03-2024-162 on the topic „Influence of structure on static and dynamic electrically conductive properties of disordered carbon“.

Conflict of interest

The authors declare that they have no conflict of interest.

References

[1] I.V. Antonets, Ye.A. Golubev, V.I. Shcheglov, A.S. Prikhodko, N.I. Borgardt. J. Phys. Chem. Solids **171**, 110994 (2022). DOI: j.jpcs.2022.110994
[2] L.S. Vieira. A review on the use of glassy carbon in advanced technological applications, Carbon **186**, 282 (2022). DOI: 10.1016/j.carbon.2021.10.022
[3] S. Sharma. Materials **11**, 1857 (2018). DOI: 10.3390/ma11101857
[4] L. Ferrer-Argemi, E.S. Aliabadi, A. Cisquella-Serra, A. Salazar, M. Madou, J. Lee. Carbon **130**, 87 (2018). DOI: 10.1016/j.carbon.2017.12.113
[5] S. Gupta, N.-H. Tai. Carbon **152**, 159 (2019). DOI: 10.1016/j.carbon.2019.06.002
[6] M. Letellier, J. Macutkevic, P. Kuzhir, J. Banys, V. Fierro, A. Celzard. Carbon **122**, 217 (2017). DOI: j.carbon.2017.06.080
[7] E.S. Belousova. Nanotechnologies Constr. Sci. Electron. J. Minsk. CNT NanoBuilding **2**, 56 (2013).
[8] N.H. Chou, N. Pierce, Y. Lei, N. Perea-López, K. Fujisawa, S. Subramanian, J.A. Robinson, G. Chen, K. Omichi, S.S. Rozhkov, N.N. Rozhkova, M. Terrones, A.R. Harutyunyan. Carbon **130**, 105 (2018). DOI: 10.1016/j.carbon.2017.12.109
[9] L. Zhang, F. Deng, X. Cheng, S. Zhang, X. Xin, Z. Liu. Fuller. Nanotub. Carbon Nanostruct. **31**, 1171 (2023). DOI: 10.1080/1536383X.2023.2259515
[10] Ye.A. Golubev, I.V. Antonets. Nanomaterials **12**, 3797 (2022). DOI: 10.3390/nano12213797
[11] J.N. Rouzaud, C. Clinard. Proc. Technol. **77–78**, 229 (2002). DOI: 10.1016/S0378-3820(02)00053-X
[12] V.V. Kovalevski, P.R. Busek, J.M. Cowley. Carbon **39**, *2*, 243 (2001). DOI: 10.1016/S0008-6223(00)00120-2
[13] I.V. Antonets, E.A. Golubev, V.I. Shcheglov. Ultramicroscopy **222**, *3*, 113212 (2021). DOI: 10.1016/j.ultramic.2021.113212
[14] I.V. Antonets, E.A. Golubev, V.I. Shcheglov. Fuller. Nanotub. Carbon Nanostruct. **32**, *3*, 246 (2024). DOI: 10.1080/1536383X.2023.2273416
[15] V.A. Ustyugov, I.V. Antonets, E.A. Golubev. Vestnik Syktyvkarskogo universiteta. Ser. 1: Matematika. Mekhanika. Informatika **53**, *4*, 69 (2024) (in Russian). DOI: 10.34130/1992-2752_2024_4_69

Translated by A.Akhtyamov